

Rate equations for Coulomb blockade with ferromagnetic leads

Stephan Braig and Piet W. Brouwer

Laboratory of Atomic and Solid State Physics, Cornell University, Ithaca, NY 14853

(Dated: September 10, 2018)

We present a density-matrix rate-equation approach to sequential tunneling through a metal particle weakly coupled to ferromagnetic leads. The density-matrix description is able to deal with correlations between degenerate many-electron states that the standard rate equation formalism in terms of occupation probabilities cannot describe. Our formalism is valid for an arbitrary number of electrons on the dot, for an arbitrary angle between the polarization directions of the leads, and with or without spin-orbit scattering on the metal particle. Interestingly, we find that the density-matrix description may be necessary even for metal particles with unpolarized leads if three or more single-electron levels contribute to the transport current and electron-electron interactions in the metal particle are described by the ‘universal interaction Hamiltonian’.

I. INTRODUCTION

Spin-polarized electron tunneling is essential to spin-based electronics¹ and nanoscale magnetics based on the spin-transfer effect.^{2,3} Whereas tunneling through a single tunnel barrier, either between two ferromagnets or between a ferromagnet and a normal metal, has been studied since the mid 1970s,⁴ the study of spin-polarized transport through mesoscopic double tunneling junctions is more recent. Double mesoscopic junctions are of interest because of the small capacitance of the central region in between the tunneling junctions, which allows electrons to be transported one by one.⁵ Experiments have been reported both for normal metal leads with a ferromagnetic island between the junctions^{6,7} and for a normal island with spin-polarized junctions.^{8,9,10} A large number of theoretical works has dealt with these cases.^{11,12,13,14,15,16,17,18,19,20,21,22,23,24,25,26,27,28,29,30}

In this work, we consider the case of a normal metal island with ferromagnetic leads. If the temperature is much larger than the tunneling rates onto or off the island, electron tunneling is sequential. In that case, quantum mechanical correlations between electrons in different states are lost because of thermal smearing, and a simple description in terms of rate equations applies. Depending on whether the temperature is small or large compared to the level spacing in the island, these rate equations describe the probability to find a certain number of electrons on the island^{31,32,33} or the occupation of the electronic states in the island.^{34,35}

Whereas the rate-equation approach was applied straightforwardly to ferromagnetic leads with collinear polarizations,^{20,28} application to leads with non-collinear polarizations requires a formulation in terms of the density matrices of degenerate levels, not the occupations of states.^{29,30} (If spin degeneracy on the normal metal island is lifted, e.g., by a magnetic field, scalar rate equations remain valid despite polarized leads.) There are two reasons for this additional complication: First, with non-collinear polarizations, no common quantization direction exists, and one cannot avoid a formulation of the problem in which electrons tunnel into superpositions of states with different spin projections.¹⁶ Second, coupling

to the ferromagnetic leads slightly lifts the spin degeneracy and leads to a slow precession of the spin on the dot.²⁹ The use of density matrices instead of occupation probabilities in the rate equation formalism allows for the inclusion of correlations between different quantum states.^{36,37} Since the temperature is much larger than the escape rate to the leads, only correlations between states with the same energy need to be taken into account.

Density-matrix rate equations were first used to describe transport through a metal particle (or a quantum dot or a single molecule) with spin-polarized tunnel contacts in a recent paper by König and Martinek²⁹ (see also Ref. 30). These authors used the Keldysh formalism to derive the density-matrix rate equations for a dot in which only one level contributes to transport. The purpose of the present work is to formulate a density-matrix rate equation for quantum dots in which many electronic levels contribute to transport and to simplify the derivation of Ref. 30. The extension to many levels is relevant for the analysis of experimental data, since the majority of experiments feature high bias voltages at which more than one electronic level contributes to the current.³⁸

A remarkable result of our study is that a formulation in terms of density-matrix rate equations is not only needed for spin-polarized leads with non-collinear polarization directions, but that it may also be necessary for unpolarized leads or for spin-polarized leads with collinear polarization directions if the metal island has a large dimensionless conductance g . These relatively large metal particles or quantum dots have degenerate or almost-degenerate many-electron levels. Correlations between the degenerate states persist during the time an electron occupies the quantum dot and need to be accounted for using a description in terms of a density matrix. The origin of the degeneracy is that in large- g metal grains or quantum dots electronic interactions are described by the ‘universal interaction Hamiltonian’.³⁹ With this interaction, many-electron levels with three or more singly occupied single-electron levels are degenerate if their spin is not maximal. For example, there are four degenerate states with three singly occupied levels and total spin $S = 1/2$. A rate equation in terms of scalar occupation probabilities only⁴⁰ will fail to describe

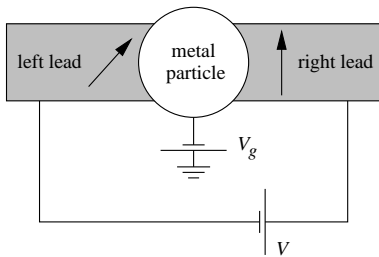


FIG. 1: Metal particle attached to two ferromagnetic leads.

correlations between these degenerate states. A detailed description of this case will be given in Sec. II C below.

II. MATRIX RATE-EQUATION FORMALISM

We consider a metal particle — or a quantum dot or a single molecule — that is attached to a number of ferromagnetic leads via tunneling contacts with a conductance much smaller than the conductance quantum e^2/h . A schematic drawing of a metal particle with two leads is shown in Fig. 1. In our formulation of the problem, we assume that all leads are fully polarized; a partially polarized lead is simply represented by two fully polarized leads with different densities of states and different tunneling rates. We assume that the temperature T is much larger than the tunneling rates to and from the leads. This is the regime for which rate equations have been shown to be a valid description of metal particles without spin-polarized leads.

A. Single doubly degenerate level

In order to make the connection to previous works,^{16,29,30} we first develop the formalism for the case of nonlinear transport through a single level. Our approach is closely connected to the works by Nazarov³⁶ and Gurvitz,³⁷ who used rate equations to describe high-bias transport through a sequence of tunnel barriers. For a metal particle in which only one level is relevant for transport, we need to consider occupation of the level by zero, one, or two electrons, at energies ε_0 , ε_1 , and ε_2 , respectively. The precise value of these energies depends

on the charging energy and exchange interaction of the metal particle, the voltages on nearby gates, etc. For occupation by zero or two electrons, the many-electron level is non-degenerate, and we can use scalars p_0 and p_2 to describe the probability to find the particle in a state with zero or two electrons, respectively. If the level is occupied by one electron only, one needs to use a 2×2 density matrix ρ_1 to fully describe the state of the particle. Conservation of probability implies

$$p_0 + \text{tr } \rho_1 + p_2 = 1. \quad (1)$$

Without tunneling to and from the reservoirs, p_0 , ρ_1 , and p_2 are time independent. The time dependence of p_0 , ρ_1 , and p_2 then arises from tunneling of electrons onto or off the metal particle: real tunneling processes shift the number of electrons on the metal particle, whereas virtual tunneling processes cause a precession of the spin if the level is singly occupied. The net tunneling rate to and from lead α depends on the direction of the polarization in that lead, which we describe by means of the spinors m_α (\bar{m}_α) pointing parallel (anti-parallel) to the polarization direction of lead α , the tunneling rate Γ_α for electrons with spin m_α , and the distribution function f_α in lead α . In order to describe both the virtual and real tunneling processes, we combine the rate Γ_α and the spinors m_α and \bar{m}_α into the spinor tunneling amplitudes

$$\gamma_\alpha = \Gamma_\alpha^{1/2} m_\alpha, \quad \bar{\gamma}_\alpha = \Gamma_\alpha^{1/2} \bar{m}_\alpha, \quad (2)$$

with $\gamma_\alpha^\dagger \gamma_\alpha = \bar{\gamma}_\alpha^\dagger \bar{\gamma}_\alpha = \Gamma_\alpha$ and $\gamma_\alpha^\dagger \bar{\gamma}_\alpha = 0$.

Virtual tunneling processes can be described by the effective Hamiltonian⁴¹

$$H_1 = \frac{\hbar}{4\pi} \text{P} \int d\xi \sum_\alpha (1 - 2f_\alpha(\xi)) \times \left[\frac{\gamma_\alpha \gamma_\alpha^\dagger}{\varepsilon_1 - \varepsilon_0 - \xi} + \frac{\bar{\gamma}_\alpha \bar{\gamma}_\alpha^\dagger}{\varepsilon_2 - \varepsilon_1 - \xi} \right], \quad (3)$$

where P denotes the Cauchy principal value. Note that if $\varepsilon_2 - \varepsilon_1 = \varepsilon_1 - \varepsilon_0$, one has H_1 proportional to the unit matrix in spin space and thus $[H_1, \rho_1] = 0$: virtual excitations do not cause a spin precession without interactions.²⁹ The time evolution of the scalars p_0 and p_2 and the 2×2 matrix ρ_1 is described by the equations^{29,30}

$$\frac{dp_0}{dt} = \sum_\alpha (1 - f_\alpha(\varepsilon_1 - \varepsilon_0)) \gamma_\alpha^\dagger \rho_1 \gamma_\alpha - \sum_\alpha f_\alpha(\varepsilon_1 - \varepsilon_0) \gamma_\alpha^\dagger p_0 \gamma_\alpha, \quad (4)$$

$$\begin{aligned} \frac{d\rho_1}{dt} &= \frac{i}{\hbar} (\rho_1 H_1 - H_1 \rho_1) + \sum_\alpha f_\alpha(\varepsilon_1 - \varepsilon_0) \gamma_\alpha p_0 \gamma_\alpha^\dagger - \frac{1}{2} \sum_\alpha (1 - f_\alpha(\varepsilon_1 - \varepsilon_0)) [\gamma_\alpha \gamma_\alpha^\dagger \rho_1 + \rho_1 \gamma_\alpha \gamma_\alpha^\dagger] \\ &\quad + \sum_\alpha (1 - f_\alpha(\varepsilon_2 - \varepsilon_1)) \bar{\gamma}_\alpha p_2 \bar{\gamma}_\alpha^\dagger - \frac{1}{2} \sum_\alpha f_\alpha(\varepsilon_2 - \varepsilon_1) [\bar{\gamma}_\alpha \bar{\gamma}_\alpha^\dagger \rho_1 + \rho_1 \bar{\gamma}_\alpha \bar{\gamma}_\alpha^\dagger], \end{aligned} \quad (5)$$

$$\frac{dp_2}{dt} = \sum_{\alpha} f_{\alpha}(\varepsilon_2 - \varepsilon_1) \bar{\gamma}_{\alpha}^{\dagger} \rho_1 \bar{\gamma}_{\alpha} - \sum_{\alpha} (1 - f_{\alpha}(\varepsilon_2 - \varepsilon_1)) \bar{\gamma}_{\alpha}^{\dagger} p_2 \bar{\gamma}_{\alpha}, \quad (6)$$

whereas the current through each of the tunnel contacts is calculated as^{34,35}

$$I_{\alpha} = f_{\alpha}(\varepsilon_1 - \varepsilon_0) \gamma_{\alpha}^{\dagger} p_0 \gamma_{\alpha} - (1 - f_{\alpha}(\varepsilon_1 - \varepsilon_0)) \gamma_{\alpha}^{\dagger} \rho_1 \gamma_{\alpha} + f_{\alpha}(\varepsilon_2 - \varepsilon_1) \bar{\gamma}_{\alpha}^{\dagger} \rho_1 \bar{\gamma}_{\alpha} - (1 - f_{\alpha}(\varepsilon_2 - \varepsilon_1)) \bar{\gamma}_{\alpha}^{\dagger} p_2 \bar{\gamma}_{\alpha}. \quad (7)$$

For $f_{\alpha} = 0$ or $f_{\alpha} = 1$, Eqs. (4)–(7) follow from considering the escape of electrons or holes from the metal particle into vacuum.^{36,37,42} The factors f_{α} and $(1 - f_{\alpha})$, which also appear in the scalar rate equations,^{34,35} are inserted to reflect the modification of tunneling rates by the electron distribution in the leads. This simple way of accounting for the presence of electrons in the leads is no longer valid when correlations between the electrons in the leads and in the metal particle are formed, such as is the case in the Kondo effect.^{22,23,24,25,26,43,44} We remark that, since Eqs. (4)–(7) are meant to describe transport at the lowest order in Γ_{α} only, the energy shift implied by the Hamiltonian H_1 need not be included in the argument of the distribution function f_{α} . For that reason, Eqs. (4)–(7) describe both the case of low bias and high bias, in contrast to the formalism of Refs. 37,42, which is appropriate for high bias only. Also note that Eqs. (4)–(6) are consistent with probability conservation, Eq. (1), and that they reduce to the standard rate equations^{34,35} once the polarizations in the leads are collinear.

B. General formalism

For the general description, we consider a normal-metal particle with many-electron levels ε_k , each of which has degeneracy j_k . The many-electron states are labeled $|k, m\rangle$, where $m = 1, \dots, j_k$. The number of electrons in state $|k, m\rangle$ is denoted by N_k . Real and virtual transitions between many-electron states are possible because of tunneling of electrons between the metal particle and the source and drain reservoirs. As before, we assume that this tunneling rate is small in comparison to the

spacing between electronic levels and temperature. In that case, we may describe the state of the dot by a set of density matrices ρ_k for each many-electron level, and we can neglect correlations between states with different energy.

The tunneling Hamiltonian describing the coupling of the metal particle to lead α is determined by the $j_k \times j_{k'}$ matrix $v_{\alpha;k,k'}^{\pm}$ containing the matrix elements between the many-electron multiplets $|k, \cdot\rangle$ and $|k', \cdot\rangle$ with $N_k = N_{k'} \pm 1$. In order to make contact to the rate equations derived above, we define the $j_k \times j_{k'}$ matrix of transition amplitudes $\gamma_{\alpha;k,k'}^{\pm} = (2\pi\nu_{\alpha}/\hbar)^{1/2} v_{\alpha;k,k'}^{\pm}$, where ν_{α} is the density of states of lead α . We define $\gamma_{\alpha;k,k'}^{\pm} = 0$ if $N_k \neq N_{k'} \pm 1$. One may write $\gamma_{\alpha;k,k'}^{\pm} = (\Gamma_{\alpha})^{1/2} w_{\alpha;k,k'}^{\pm}$, where $w_{\alpha;k,k'}^{\pm}$ is dimensionless and Γ_{α} is the tunneling rate through contact α if the metal island is replaced by an electron reservoir. For point contacts, the magnitude of $w_{\alpha;k,k'}^{\pm}$ is set by the value of a wavefunction at the location of the contact.⁴⁵ If the degeneracy of the multiplets $|k, \cdot\rangle$ and $|k', \cdot\rangle$ arises from angular momentum, the matrix structure of $w_{\alpha;k,k'}^{\pm}$ is set by the Clebsch-Gordon coefficients. With this notation, virtual excitations lead to the effective Hamiltonian H_k for the multiplet $|k, \cdot\rangle$,

$$H_k = \frac{\hbar}{4\pi} \text{P} \int d\xi \sum_{\alpha,k'} (1 - 2f_{\alpha}(\xi)) \times \left[\frac{\gamma_{\alpha;k,k'}^+ \gamma_{\alpha;k',k}^-}{\varepsilon_k - \varepsilon_{k'} - \xi} + \frac{\gamma_{\alpha;k,k'}^- \gamma_{\alpha;k',k}^+}{\varepsilon_{k'} - \varepsilon_k - \xi} \right]. \quad (8)$$

Then the appropriate generalization of the rate equations (4)–(6) and the current formula (7) is

$$\begin{aligned} \frac{\partial \rho_k}{\partial t} = & \frac{i}{\hbar} (\rho_k H_k - H_k \rho_k) + \sum_{\alpha,k'} \left[f_{\alpha}(\varepsilon_k - \varepsilon_{k'}) \gamma_{\alpha;k,k'}^+ \rho_{k'} \gamma_{\alpha;k',k}^- + (1 - f_{\alpha}(\varepsilon_{k'} - \varepsilon_k)) \gamma_{\alpha;k,k'}^- \rho_{k'} \gamma_{\alpha;k',k}^+ \right] \\ & - \frac{1}{2} \sum_{\alpha,k} \left[f_{\alpha}(\varepsilon_{k'} - \varepsilon_k) (\gamma_{\alpha;k,k'}^- \gamma_{\alpha;k',k}^+ \rho_k + \rho_k \gamma_{\alpha;k,k'}^- \gamma_{\alpha;k',k}^+) \right. \\ & \left. + (1 - f_{\alpha}(\varepsilon_k - \varepsilon_{k'})) (\gamma_{\alpha;k,k'}^+ \gamma_{\alpha;k',k}^- \rho_k + \rho_k \gamma_{\alpha;k,k'}^+ \gamma_{\alpha;k',k}^-) \right], \quad (9) \end{aligned}$$

$$I_{\alpha} = e \sum_{k,k'} \left[f_{\alpha}(\varepsilon_k - \varepsilon_{k'}) \gamma_{\alpha;k,k'}^+ \rho_{k'} \gamma_{\alpha;k',k}^- - (1 - f_{\alpha}(\varepsilon_{k'} - \varepsilon_k)) \gamma_{\alpha;k,k'}^- \rho_{k'} \gamma_{\alpha;k',k}^+ \right]. \quad (10)$$

Here the summation over k' extends over all many-

electron states different from k . One easily verifies that

Eq. (9) conserves the total probability $\sum_k \text{tr } \rho_k = 1$.

C. Unpolarized leads

The density-matrix rate equations (9) and (10) do *not* necessarily reduce to the standard scalar rate equations of Refs. 34,35 when all leads are unpolarized or when the leads have collinear spin polarizations. The reason for this, at first, surprising fact is that overlaps between different many-body states are not accurately described by scalar transition probabilities if there are degeneracies. With degeneracies, non-orthogonal coherent superpositions of many-electron states are involved in the transport process.

Although level repulsion rules out degeneracies in the single-particle states in a generic metal grain or quantum dot, for large metal grains or quantum dots, (near) degeneracies may occur in the many-electron spectrum. The origin of the degeneracy is that electron-electron interactions in metal particles or quantum dots with large dimensionless conductance g are described by the ‘universal interaction Hamiltonian’,³⁹

$$H_{ee} = E_C N^2 + JS^2, \quad (11)$$

where N is the total number of electrons on the metal particle, E_C is the charging energy, S is the total spin, and J is the exchange interaction strength. According to Eq. (11), the energy of a many-electron state depends on the occupation of the single-electron states and the total spin S only. This gives rise to degeneracies in many-electron states with three or more singly occupied single-electron levels. For example, in a metal grain with single-electron levels labeled 1, 2, and 3, the two states

$$|+\rangle \equiv \frac{1}{\sqrt{3}} \left(e^{\frac{2\pi i}{3}} c_{\uparrow 1}^\dagger c_{\downarrow 2}^\dagger c_{\downarrow 3}^\dagger |0\rangle + e^{-\frac{2\pi i}{3}} c_{\downarrow 1}^\dagger c_{\uparrow 2}^\dagger c_{\downarrow 3}^\dagger |0\rangle + c_{\downarrow 1}^\dagger c_{\downarrow 2}^\dagger c_{\uparrow 3}^\dagger |0\rangle \right), \quad (12a)$$

$$|-\rangle \equiv \frac{1}{\sqrt{3}} \left(e^{-\frac{2\pi i}{3}} c_{\uparrow 1}^\dagger c_{\downarrow 2}^\dagger c_{\downarrow 3}^\dagger |0\rangle + e^{\frac{2\pi i}{3}} c_{\downarrow 1}^\dagger c_{\uparrow 2}^\dagger c_{\downarrow 3}^\dagger |0\rangle + c_{\downarrow 1}^\dagger c_{\downarrow 2}^\dagger c_{\uparrow 3}^\dagger |0\rangle \right), \quad (12b)$$

both have three singly occupied single-electron levels with total spin $S = 1/2$ and $S_z = -1/2$. Hence, according to the ‘universal interaction Hamiltonian’, they are degenerate. Since both states have the same value of S_z , the degeneracy is not broken by a magnetic field. However, in principle it may be lifted by non-universal residual interactions that are not included in the ‘universal interaction Hamiltonian’,³⁹ but such residual interactions are weak if $g \gg 1$, and they can be neglected if the level splitting that they cause is smaller than the level broadening due to escape through the tunnel contacts. The degeneracy may also be lifted in metal particles with spin-orbit scattering if the spin-orbit rate \hbar/τ_{so} is comparable to the mean spacing Δ between single-electron levels.^{46,47}

We now illustrate how this degeneracy necessitates the use of a matrix rate equation using the example of a metal particle with three spin-degenerate single-electron levels. For the ease of argument, a magnetic field is applied along the negative z axis. We consider transitions from the three two-electron states with $S = 1$, $S_z = -1$,

$$|1\rangle \equiv c_{\downarrow 2}^\dagger c_{\downarrow 3}^\dagger |0\rangle, \quad (13a)$$

$$|2\rangle \equiv c_{\downarrow 1}^\dagger c_{\downarrow 3}^\dagger |0\rangle, \quad (13b)$$

$$|3\rangle \equiv c_{\downarrow 1}^\dagger c_{\downarrow 2}^\dagger |0\rangle, \quad (13c)$$

to the degenerate three-electron states (12). As the states (13) are non-degenerate, they are described by means of the probability p_j of finding the system in state $|j\rangle$, $j = 1, 2, 3$. On the other hand, the states (12) are degenerate and we need to describe their occupation by a 2×2 density matrix ρ ,

$$\rho = \begin{pmatrix} \rho_{++} & \rho_{+-} \\ \rho_{-+} & \rho_{--} \end{pmatrix}. \quad (14)$$

Transitions from the states (13) to the doublet (12) occur at rates Γ_j , $j = 1, 2, 3$. Writing down the time evolution of ρ that results from those transitions, we find

$$\frac{d\rho}{dt} = \frac{\Gamma_1}{3} p_1 \begin{pmatrix} 1 & e^{\frac{2\pi i}{3}} \\ e^{-\frac{2\pi i}{3}} & 1 \end{pmatrix} + \frac{\Gamma_2}{3} p_2 \begin{pmatrix} 1 & e^{-\frac{2\pi i}{3}} \\ e^{\frac{2\pi i}{3}} & 1 \end{pmatrix} + \frac{\Gamma_3}{3} p_3 \begin{pmatrix} 1 & 1 \\ 1 & 1 \end{pmatrix} + \dots, \quad (15)$$

where the remaining terms describe processes that do not depend on the p_j , $j = 1, 2, 3$. Clearly, there is no basis that would diagonalize all three matrices in Eq. (15) simultaneously for arbitrary choice of the p_j . This proves that it is imperative to use the full matrix structure for ρ in order to properly deal with correlations between the states (12).

III. APPLICATION TO SPIN-POLARIZED TRANSPORT

We now apply the formalism of the previous section to transport through metal particles with ferromagnetic contacts. We first consider the simpler case of a metal particle in which only one energy level participates in transport, and then consider the case of multiple levels.

A. Single doubly occupied level

The linear-response conductance G of a metal particle coupled to two fully polarized ferromagnetic leads, labeled L and R, is easily calculated from Eqs. (4)-(7),

$$G = G_0 \cos^2(\theta/2) \left[1 - \frac{4a^2 \Gamma_L \Gamma_R \sin^2(\theta/2)}{[a^2 + (1 - f(\varepsilon_1 - \varepsilon_0) + f(\varepsilon_2 - \varepsilon_1))^2] (\Gamma_L + \Gamma_R)^2} \right]^{-1}, \quad (16)$$

where θ is the angle between the polarizations of the ferromagnets, G_0 is the linear conductance for $\theta \rightarrow 0$,

$$G_0 = \frac{e^2}{\hbar T} \frac{\Gamma_L \Gamma_R (1 - f(\varepsilon_2 - \varepsilon_1)) f(\varepsilon_1 - \varepsilon_0) (1 - f(\varepsilon_1 - \varepsilon_0) + f(\varepsilon_2 - \varepsilon_1))}{(\Gamma_L + \Gamma_R) (1 + f(\varepsilon_1 - \varepsilon_0) - f(\varepsilon_2 - \varepsilon_1))}, \quad (17)$$

and

$$a = P \int \frac{d\xi}{2\pi} \frac{(1 - 2f(\xi))(\varepsilon_2 + \varepsilon_0 - 2\varepsilon_1)}{(\varepsilon_1 - \varepsilon_0 - \xi)(\varepsilon_2 - \varepsilon_1 - \xi)}. \quad (18)$$

For partially polarized leads with polarization $P_\alpha \equiv (\Gamma_\alpha - \bar{\Gamma}_\alpha)/(\Gamma_\alpha + \bar{\Gamma}_\alpha)$, where $\bar{\Gamma}_\alpha$ is the tunneling rate for electrons with spin \bar{m}_α , one finds

$$G = \frac{2G_0}{D} \left[\Gamma_L(1 - P_L) + \Gamma_R(1 - P_R) + \frac{P_L^2 P_R^2 \Gamma_L \Gamma_R \sin^2 \theta}{\Gamma_L(1 + P_R) + \Gamma_R(1 + P_L) - DE} \right], \quad (19)$$

where G_0 is given by Eq. (17) above, and we abbreviated

$$D = \Gamma_R(1 + P_L)(1 - P_R) + \Gamma_L(1 - P_L)(1 + P_R) + 4\Gamma_L \Gamma_R P_L P_R \sin^2(\theta/2)/(\Gamma_L + \Gamma_R),$$

$$E = a^2(1 + P_L)(1 + P_R)(\Gamma_L + \Gamma_R)[a^2 + (1 - f(\varepsilon_1 - \varepsilon_0) + f(\varepsilon_2 - \varepsilon_1))^2]^{-1}[\Gamma_L(1 + P_R) + \Gamma_R(1 + P_L)]^{-1}.$$

For symmetric contacts, $\Gamma_L = \Gamma_R$ and $P_L = P_R$, Eqs. (16) and (19) were previously obtained in Refs. 29, 30. Without the spin-precession term (the first term on the r.h.s. of Eq. (5)), we recover the linear conductance calculated by Usaj and Baranger,¹⁶ after correction of a technical mistake in Ref. 16.

As pointed out by König and Martinek, the role of the spin-precession term is to reduce the angular dependence of the conductance. Our general results (16) and (19) show how this reduction depends on the symmetry of the contacts: the reduction is strongest for symmetric contacts ($\Gamma_R = \Gamma_L$), whereas it vanishes in the generic case of very asymmetric contacts ($\Gamma_R \ll \Gamma_L$). In the latter case, the spin precession axis is aligned with m_L ; precession around m_L does not change the angular dependence of the conductance.

B. Case of up to three electrons on the dot

For a metal particle in which more than one level contributes to transport we calculated the differential conductance $G = \partial I / \partial V$ numerically as a function of the bias voltage V .

The numerical calculation was done for a metal particle in which five single-electron levels, with a total of two or three electrons, contributed to the current. The lead polarizations were chosen parallel or anti-parallel, with polarizations $P_L = P_R \equiv P$. With a maximum of three singly-occupied levels, the largest possible spin on the dot was $3/2$. The positions of the single-electron

energy levels were taken from the center of a matrix drawn from the Gaussian Orthogonal Ensemble of random matrix theory, and the temperature T was set at one percent of the mean spacing Δ between the single-electron levels, to ensure that all features in the current-voltage characteristic could be resolved in the numerical calculation. Electron-electron interactions were described using Eq. (11). In the numerical calculations, we set $E_C = 25\Delta$, and $J = -0.32\Delta$. (Values of the exchange constant J are tabulated in Ref. 47 for most normal metals.) The tunneling rates Γ_L and Γ_R were chosen $\lesssim 0.1k_B T$ and equal for all levels, as is appropriate for metal particles with wide tunnel barriers. The source-drain voltage V was applied to the right lead and was assumed to change the effective chemical potential in the right lead only.

The use of leads with collinear polarizations in the numerical calculations eliminates most of the necessity of using density-matrix rate equations, except for the degenerate $S = 1/2$ states with three singly-occupied levels. These states are fourfold degenerate. We denote them

$$|\frac{1}{2}, +\rangle \equiv \frac{1}{\sqrt{3}}(e^{\frac{2\pi i}{3}} |\uparrow\uparrow\downarrow\rangle + e^{-\frac{2\pi i}{3}} |\uparrow\downarrow\uparrow\rangle + |\downarrow\uparrow\uparrow\rangle), \quad (20a)$$

$$|\frac{1}{2}, -\rangle \equiv \frac{1}{\sqrt{3}}(e^{-\frac{2\pi i}{3}} |\uparrow\uparrow\downarrow\rangle + e^{\frac{2\pi i}{3}} |\uparrow\downarrow\uparrow\rangle + |\downarrow\uparrow\uparrow\rangle), \quad (20b)$$

$$|-\frac{1}{2}, +\rangle \equiv \frac{1}{\sqrt{3}}(e^{\frac{2\pi i}{3}} |\uparrow\downarrow\downarrow\rangle + e^{-\frac{2\pi i}{3}} |\downarrow\uparrow\downarrow\rangle + |\downarrow\downarrow\uparrow\rangle), \quad (21a)$$

$$|-\frac{1}{2}, -\rangle \equiv \frac{1}{\sqrt{3}}(e^{-\frac{2\pi i}{3}} |\uparrow\downarrow\downarrow\rangle + e^{\frac{2\pi i}{3}} |\downarrow\uparrow\downarrow\rangle + |\downarrow\downarrow\uparrow\rangle). \quad (21b)$$

However, only the twofold degeneracy inside the pairs with $S_z = 1/2$ and $S_z = -1/2$ is relevant, and it is sufficient to describe the occupation of the four $S = 1/2$ states with two 2×2 density matrices $\rho(S_z = 1/2)$ and $\rho(S_z = -1/2)$ as in Eq. (14).

To illustrate the use of the matrix rate equations in this case, we write down the full transition vectors for the transition between the $S = 1$ triplet states and the two doublets (20) and (21). We denote the $S = 1$ triplet state by $|S_z\rangle$, with $S_z = -1, 0, 1$. In relation to the two energy levels already occupied in the triplet state, we consider adding an electron in a single-electron level with higher, lower, or intermediate energy and denote the different vectors by superscripts h , l , and m , respectively. Choosing the orientation of the leads as the spin quantization axis, the nonzero transition vectors for addition of an electron with spin up from lead α as they appear in the rate equation (9) are $\gamma_\alpha^{+,h} = (\Gamma_\alpha^h)^{1/2} w^{+,h}$, $\gamma_\alpha^{+,l} = (\Gamma_\alpha^l)^{1/2} w^{+,l}$, and $\gamma_\alpha^{+,m} = (\Gamma_\alpha^m)^{1/2} w^{+,m}$, with

$$w_{|\frac{1}{2}\rangle,|0\rangle}^{+,h} = \frac{-1}{\sqrt{6}} \begin{pmatrix} e^{-2\pi i/3} \\ e^{2\pi i/3} \end{pmatrix}, \quad (22a)$$

$$w_{|-\frac{1}{2}\rangle,|-1\rangle}^{+,h} = \frac{1}{\sqrt{3}} \begin{pmatrix} 1 \\ 1 \end{pmatrix}, \quad (22b)$$

$$w_{|\frac{1}{2}\rangle,|0\rangle}^{+,l} = \frac{-1}{\sqrt{6}} \begin{pmatrix} 1 \\ 1 \end{pmatrix}, \quad (22c)$$

$$w_{|-\frac{1}{2}\rangle,|-1\rangle}^{+,l} = \frac{1}{\sqrt{3}} \begin{pmatrix} e^{-2\pi i/3} \\ e^{2\pi i/3} \end{pmatrix}, \quad (22d)$$

$$w_{|\frac{1}{2}\rangle,|0\rangle}^{+,m} = \frac{1}{\sqrt{6}} \begin{pmatrix} e^{2\pi i/3} \\ e^{-2\pi i/3} \end{pmatrix}, \quad (22e)$$

$$w_{|-\frac{1}{2}\rangle,|-1\rangle}^{+,m} = \frac{1}{\sqrt{3}} \begin{pmatrix} e^{2\pi i/3} \\ e^{-2\pi i/3} \end{pmatrix}. \quad (22f)$$

The transition vectors for adding a spin-down electron follow straightforwardly from the above. The amplitudes for removing electrons are obtained from the above by hermitian conjugation. Although these were not considered in the numerical calculations, we mention that the overlap matrices for non-collinear lead polarizations can be obtained from Eqs. (22) by combining the transition vectors into 4×3 matrix amplitudes for the full transition from the spin-1 triplet to the three-electron spin- $\frac{1}{2}$ quadruplet, followed by multiplication with appropriate representations of rotation matrices. In this particular case, the transition matrix amplitude would have to be multiplied with a four-dimensional representation from the left and a three-dimensional representation from the right. The relevant rotation matrices are listed in the appendix.

We now turn to the results of our numerical calculations. One expects that anti-parallel lead polarizations cause spin accumulation on the metal island. This can indeed be observed in our solution of the rate equations, as shown in Fig. 2, where we plot the probability of finding spin $S = 3/2$ (as opposed to $S = 1/2$) on the metal particle for different lead polarizations P . For anti-parallel

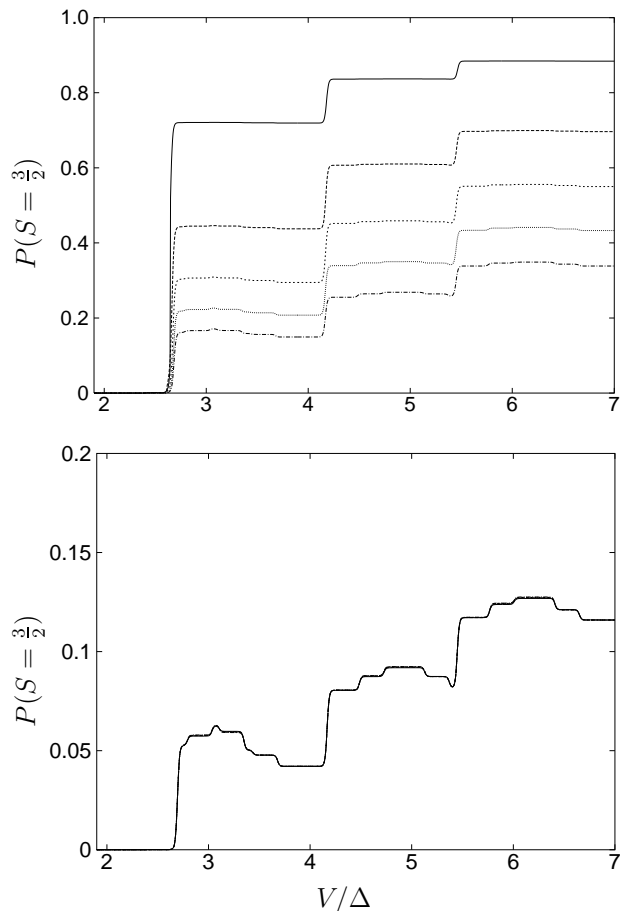


FIG. 2: Probability of finding total spin $3/2$ on the dot for anti-parallel (top panel) and parallel lead polarizations (bottom panel) featuring polarizations $P=P_L=P_R=0.95, 0.85, 0.75, 0.65, 0.55$ (top to bottom), with $\Gamma_R/\Gamma_L = 0.2$.

lead polarizations, the probability to find $S = 3/2$ increases with increasing polarization, whereas it is virtually independent of polarization for parallel lead polarizations.

In Figs. 3 and 4 we address the dependence of peaks of the differential conductance on the lead polarization P . The figure describes both parallel lead polarizations (positive P in the figure) and anti-parallel lead polarizations (negative P in the figure). Some peaks evolve non-monotonously, whereas others rise or fall monotonously in magnitude. Of particular interest are those conductance peaks that evolve from positive to negative values. Negative conductance peaks at voltage V arise if, upon reaching that voltage, a many-body state that is poorly connected to other states is made accessible. (This type of behavior is not limited to ferromagnetic leads.) Not only does there seem to be a tendency toward negative differential conductance upon going from anti-parallel to parallel leads but also when making the transition from $\Gamma_R \ll \Gamma_L$ to a more symmetric coupling $\Gamma_R \sim \Gamma_L$, as shown in Fig. 4. In general, conductance peak spectra for a different polarization orientation can therefore look

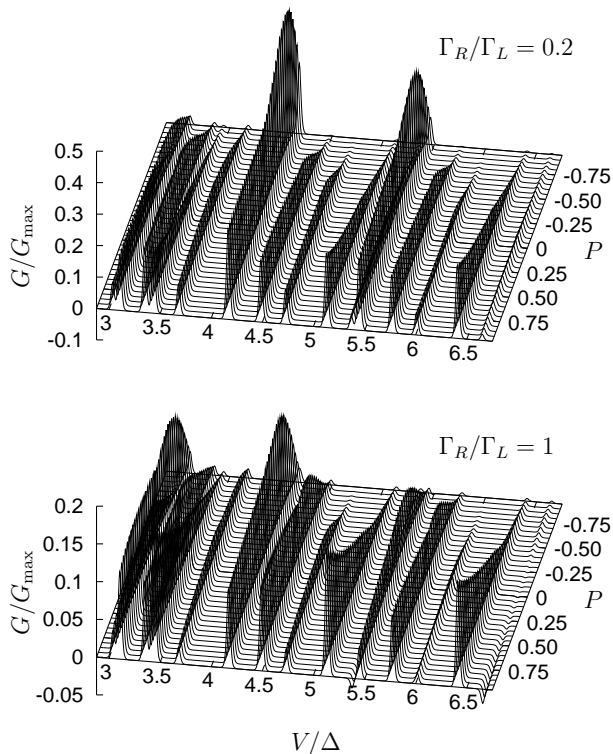


FIG. 3: Excerpt from the spectrum of several conductance peaks for anti-parallel and parallel lead orientations as a function of source-drain voltage V (in units of the mean level spacing Δ) and of lead polarization $P = P_L = P_R$. For ease of presentation, the case of parallel polarization is plotted against *negative* polarization. The excerpt shown here does not include the dominant low-energy peak.

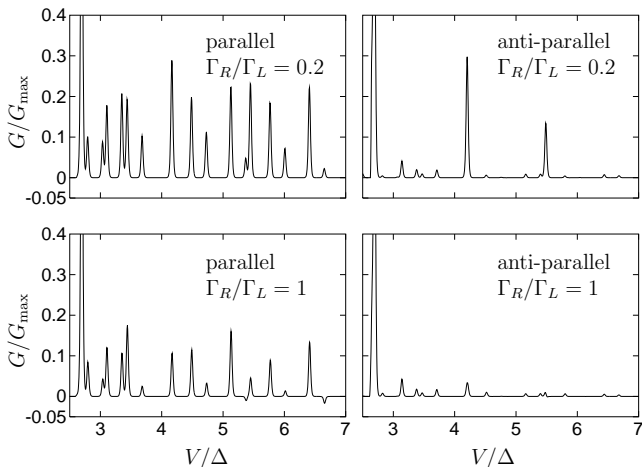


FIG. 4: Normalized differential conductance as a function of source-drain voltage V for parallel (left panels) and anti-parallel (right panels) lead polarizations $P = P_L = P_R = 0.9$. The vertical scale has been normalized to the magnitude G_{\max} of the largest (first) conductance peak.

very different in terms of both position and magnitude of the most dominant peaks, even if recorded for the same sample.

IV. INFLUENCE OF SPIN-ORBIT SCATTERING

The role of spin-orbit scattering inside the metal particle is best illustrated by considering the case of transport through one doubly (Kramers) degenerate level. (Spin-orbit scattering in the reservoirs instead of in the metal island was considered in Ref. 48.) With spin-orbit scattering, the two eigenfunctions of the level are spinor wavefunctions. Once the spin quantization axes are fixed at a reference point in the metal particle, the two spinor wavefunctions define a spatially dependent spin quantization axis in the metal particle. The spinors m_α and \bar{m}_α that define directions parallel and anti-parallel to the polarization direction in lead α are defined with respect to the quantization axis at the contact with lead α . Hence, the presence of spin orbit scattering in the normal metal particle alters the spinor structure of the transition amplitudes γ_α , but it does not change the general structure of the rate equations. The same conclusions hold for the general case.

The above considerations imply that, for a metal particle coupled to ferromagnetic source and drain reservoirs via two *point* contacts and with only a *single* level contributing to transport, the sole effect of spin-orbit scattering is a sample-specific shift of the angle between the polarizations in the two leads. On the other hand, for a metal particle coupled to source and drain leads via many-channel tunneling contacts, or for a metal particle in which more than one level contributes to transport, the effect of spin-orbit scattering is more complicated since different levels and different channels experience different rotations of the spin reference frame. In particular, with strong spin-orbit scattering, (spin) transport through different channels or through different levels will involve completely different rotation angles, so that the effective degree of spin polarization in the junction is greatly reduced. In the limit of a large number of channels and strong spin-orbit scattering, the rate equations in fact reduce to the unpolarized case.

V. CONCLUSION

We have extended the rate-equation formalism to the case of a normal island (metal nanoparticle, quantum dot, or single molecule) attached to spin-polarized contacts with non-collinear polarization directions. Our formalism provides a transparent description of the sequential tunneling process in this system, and is suitable for applications to both linear and nonlinear transport.

Whether one has to employ matrix rate equations or the simpler scalar rate equations is determined by the

symmetries and energy degeneracies of the metal island and the leads. We distinguish the following cases: (i) leads and island have the same symmetries and degeneracies, (ii) some symmetries present on the island are broken in the leads, and (iii) leads and island feature the same symmetries but there are additional degeneracies on the dot. Case (i) corresponds, *e.g.*, to a normal-metal island with unpolarized leads and spin-degenerate energy levels on the dot, or to a normal-metal metal island with spin-polarized leads with collinear polarization directions. In that case, the standard rate equations of Refs. 34,35 are applicable if there are no further degeneracies on the island. Case (i) also describes spin-polarized leads with non-collinear polarization directions if spin degeneracy on the island is lifted by a magnetic field, be it an applied field or the stray field of the ferromagnetic leads. In contrast, the other two situations require matrix rate equations: Case (ii) applies to normal metal particles with ferromagnetic leads that are polarized in non-collinear directions so that tunneling occurs into coherent superpositions of states on the dot. The additional degeneracies required for case (iii) arise in the many-electron spectrum of generic metal particles with or without spin-polarized leads if the ‘universal interaction Hamiltonian’ describes the electron-electron interactions on the metal particle. Such degeneracies can be lifted by non-universal interaction corrections if the resulting energy splitting is larger than the level broadening due to escape to the leads. These corrections scale as $1/g$, where g is the dimensionless conductance of the metal particle, and as a consequence, the larger the size of the normal-metal island, the more important the use of matrix rate equations becomes.

Acknowledgments

We would like to thank H. U. Baranger, K. Flensberg, J. Martinek, D. C. Ralph, and G. Usaj for discussions. This work was supported by the Cornell Center for Materials Research under NSF grant no. DMR 0079992, by the NSF under grant no. DMR 0334499, and by the Packard

foundation.

APPENDIX: ROTATION MATRICES

This appendix contains the rotation matrices for transformation from the basis aligned with the quantization axis to a basis forming a relative angle θ with the original quantization axis. We restrict ourselves to the case of up to three electrons on the dot, so that we only need representations up to dimensionality four. (The four-dimensional representations correspond to the quadruplets of total spin $S = 3/2$ and $S = 1/2$ in the case of three singly-occupied single-electron levels.) Also, we only consider polarizations in the xz plane, so that any superposition of single spins can be expressed in terms of real coefficients.

1. Two dimensions: spin-1/2 doublet

In the standard basis of spin up and spin down,

$$(1, 0) \equiv |\uparrow\rangle, \quad (0, 1) \equiv |\downarrow\rangle, \quad (\text{A.1})$$

the rotation matrix is

$$R_2 = \begin{pmatrix} \cos(\theta) & \sin(\theta) \\ -\sin(\theta) & \cos(\theta) \end{pmatrix}. \quad (\text{A.2})$$

2. Three dimensions: spin-1 triplet

In the basis created by successively applying the spin-lowering operator S_- to $|\uparrow\uparrow\rangle$,

$$\begin{aligned} (1, 0, 0) &\equiv |\uparrow\uparrow\rangle, \\ (0, 1, 0) &\equiv (|\uparrow\downarrow\rangle + |\downarrow\uparrow\rangle)/\sqrt{2}, \\ (0, 0, 1) &\equiv |\downarrow\downarrow\rangle, \end{aligned} \quad (\text{A.3})$$

the rotation matrix reads

$$R_3 = \begin{pmatrix} \cos^2(\theta) & \sqrt{2}\cos(\theta)\sin(\theta) & \sin^2(\theta) \\ -\sqrt{2}\cos(\theta)\sin(\theta) & \cos^2(\theta) - \sin^2(\theta) & \sqrt{2}\cos(\theta)\sin(\theta) \\ \sin^2(\theta) & -\sqrt{2}\cos(\theta)\sin(\theta) & \cos^2(\theta) \end{pmatrix}. \quad (\text{A.4})$$

3. Four dimensions: spin-3/2 quadruplet

The maximum spin-3/2 states feature electrons in three singly occupied single-electron levels. In the basis obtained by successively applying the spin-lowering operator S_- to $|\uparrow\uparrow\uparrow\rangle$,

$$\begin{aligned} (1, 0, 0, 0) &\equiv |\uparrow\uparrow\uparrow\rangle, & (0, 1, 0, 0) &\equiv (|\uparrow\uparrow\downarrow\rangle + |\uparrow\downarrow\uparrow\rangle + |\downarrow\uparrow\uparrow\rangle)/\sqrt{3}, \\ (0, 0, 1, 0) &\equiv (|\uparrow\downarrow\downarrow\rangle + |\downarrow\uparrow\downarrow\rangle + |\downarrow\downarrow\uparrow\rangle)/\sqrt{3}, & (0, 0, 0, 1) &\equiv |\downarrow\downarrow\downarrow\rangle, \end{aligned} \quad (\text{A.5})$$

we obtain the following rotation matrix

$$R_{4, \frac{3}{2}} = \begin{pmatrix} \cos^3(\theta) & \sqrt{3} \cos^2(\theta) \sin(\theta) & \sqrt{3} \cos(\theta) \sin^2(\theta) & \sin^3(\theta) \\ -\sqrt{3} \cos^2(\theta) \sin(\theta) & \cos^3(\theta) - 2 \cos(\theta) \sin^2(\theta) & -\sin^3(\theta) + 2 \cos^2(\theta) \sin(\theta) & \sqrt{3} \cos(\theta) \sin^2(\theta) \\ \sqrt{3} \cos(\theta) \sin^2(\theta) & \sin^3(\theta) - 2 \cos^2(\theta) \sin(\theta) & \cos^3(\theta) - 2 \cos(\theta) \sin^2(\theta) & \sqrt{3} \cos^2(\theta) \sin(\theta) \\ -\sin^3(\theta) & \sqrt{3} \cos(\theta) \sin^2(\theta) & -\sqrt{3} \cos^2(\theta) \sin(\theta) & \cos^3(\theta) \end{pmatrix}. \quad (\text{A.6})$$

4. Four dimensions: spin-1/2 quadruplet

For the four-fold degenerate many-electron state with total spin $S = 1/2$ and three singly occupied single-electron levels, we write the rotation matrix in the basis

$$\begin{aligned} (1, 0, 0, 0) &\equiv (e^{\frac{2\pi i}{3}} |\uparrow\uparrow\downarrow\rangle + e^{-\frac{2\pi i}{3}} |\uparrow\downarrow\uparrow\rangle + |\downarrow\uparrow\uparrow\rangle)/\sqrt{3}, & (0, 1, 0, 0) &\equiv (e^{-\frac{2\pi i}{3}} |\uparrow\uparrow\downarrow\rangle + e^{\frac{2\pi i}{3}} |\uparrow\downarrow\uparrow\rangle + |\downarrow\uparrow\uparrow\rangle)/\sqrt{3}, \\ (0, 0, 1, 0) &\equiv (e^{\frac{2\pi i}{3}} |\uparrow\downarrow\downarrow\rangle + e^{-\frac{2\pi i}{3}} |\downarrow\uparrow\downarrow\rangle + |\downarrow\downarrow\uparrow\rangle)/\sqrt{3}, & (0, 0, 0, 1) &\equiv (e^{-\frac{2\pi i}{3}} |\uparrow\downarrow\downarrow\rangle + e^{\frac{2\pi i}{3}} |\downarrow\uparrow\downarrow\rangle + |\downarrow\downarrow\uparrow\rangle)/\sqrt{3}. \end{aligned} \quad (\text{A.7})$$

The first two vectors have $S_z = 1/2$, the other two have $S_z = -1/2$. In this basis, the rotation matrix then reads

$$R_{4, \frac{1}{2}} = \begin{pmatrix} 0 & \cos(\theta) & -\frac{1}{2} \sin(\theta) e^{\frac{2\pi i}{3}} & 0 \\ \cos(\theta) & 0 & 0 & -\frac{1}{2} \sin(\theta) e^{-\frac{2\pi i}{3}} \\ \frac{1}{2} \sin(\theta) e^{\frac{2\pi i}{3}} & 0 & 0 & \cos(\theta) \\ 0 & \frac{1}{2} \sin(\theta) e^{-\frac{2\pi i}{3}} & \cos(\theta) & 0 \end{pmatrix}. \quad (\text{A.8})$$

-
- ¹ I. Žutić, J. Fabian, and S. D. Sarma, *Rev. Mod. Phys.* **76**, 323 (2004).
² L. Berger, *Phys. Rev. B* **54**, 9353 (1996).
³ J. C. Slonczewski, *J. Magn. Magn. Mater.* **159**, 1 (1996).
⁴ M. Jullière, *Phys. Lett. A* **54**, 225 (1975).
⁵ H. Grabert and M. H. Devoret, eds., *Single Charge Tunneling*, vol. 294 of *Nato ASI Series B* (Plenum, New York, 1992).
⁶ S. Guéron, M. M. Deshmukh, E. B. Myers, and D. C. Ralph, *Phys. Rev. Lett.* **83**, 4148 (1999).
⁷ M. M. Deshmukh, S. Kleff, S. Guéron, E. Bonet, A. N. Pasupathy, J. von Delft, and D. C. Ralph, *Phys. Rev. Lett.* **87**, 226801 (2001).
⁸ M. M. Deshmukh and D. C. Ralph, *Phys. Rev. Lett.* **89**, 266803 (2002).
⁹ R. M. Potok, J. A. Folk, C. M. Marcus, V. Umansky, M. Hanson, and A. C. Gossard, *Phys. Rev. Lett.* **91**, 016802 (2003).
¹⁰ A. Pasupathy, R. Białczak, J. Martinek, J. Grose, L. Donev, P. McEuen, and D. C. Ralph, preprint (2004).
¹¹ J. Barnaś and A. Fert, *Phys. Rev. Lett.* **80**, 1058 (1998).
¹² S. Takahashi and S. Maekawa, *Phys. Rev. Lett.* **80**, 1758 (1998).
¹³ A. Brataas, Y. V. Nazarov, J. Inoue, and G. E. W. Bauer, *Phys. Rev. B* **59**, 93 (1999).
¹⁴ J. Barnaś, J. Martinek, G. Michalek, B. R. Bulka, and A. Fert, *Phys. Rev. B* **62**, 12363 (2000).
¹⁵ W. Rudzinski and J. Barnaś, *Phys. Rev. B* **64**, 085318 (2001).
¹⁶ G. Usaj and H. U. Baranger, *Phys. Rev. B* **63**, 184418 (2001).
¹⁷ J. Martinek, J. Barnaś, S. Maekawa, H. Schoeller, and G. Schön, *Phys. Rev. B* **66**, 014402 (2002).
¹⁸ N. Sergueev, Q. feng Sun, H. Guo, B. G. Wang, and J. Wang, *Phys. Rev. B* **65**, 165303 (2002).
¹⁹ J. Fransson, O. Eriksson, and I. Sandalov, *Phys. Rev. Lett.* **88**, 226601 (2002).
²⁰ A. Cottet, W. Belzig, and C. Bruder, *Phys. Rev. Lett.* **92**, 206801 (2004); A. Cottet, W. Belzig, and C. Bruder, *Phys. Rev. B* **70**, 115315 (2004).
²¹ A. Cottet and W. Belzig, *Europhys. Lett.* **66**, 405 (2004).
²² J. Ma and X. L. Lei, *Europhys. Lett.* **67**, 432 (2004).
²³ J. Martinek, Y. Utsumi, H. Imamura, J. Barnaś, S. Maekawa, J. König, and G. Schön, *Phys. Rev. Lett.* **91**, 127203 (2003).
²⁴ J. Martinek, M. Sindel, L. Borda, J. Barnaś, J. König, G. Schön, and J. von Delft, *Phys. Rev. Lett.* **91**, 247202 (2003).
²⁵ M.-S. Choi, D. Sánchez, and R. López, *Phys. Rev. Lett.* **92**, 056601 (2004) **92**, 056601 (2004).
²⁶ J. Martinek, M. Sindel, L. Borda, J. Barnaś, R. Bulla, J. König, G. Schön, S. Maekawa, and J. von Delft, *cond-mat/0406323* (2004).
²⁷ J. N. Pedersen, J. Q. Thomassen, and K. Flensberg, *cond-mat* (2004).
²⁸ X. Waintal and P. W. Brouwer, *Phys. Rev. Lett.* **91**, 247201 (2003).
²⁹ J. König and J. Martinek, *Phys. Rev. Lett.* **90**, 166602 (2003).
³⁰ M. Braun, J. König, and J. Martinek, *Phys. Rev. B* **70**, 195345 (2004).
³¹ R. I. Shekhter, *Zh. Eksp. Teor. Fiz.* **63**, 1410 (1972), [*Sov. Phys. JETP* **36**, 747 (1973)].
³² I. O. Kulik and R. I. Shekhter, *Zh. Eksp. Teor. Fiz.* **68**, 623 (1975), [*Sov. Phys. JETP* **41**, 308 (1975)].
³³ D. V. Averin and K. K. Likharev, *J. Low Temp. Phys.* **62**,

- 345 (1986).
- ³⁴ C. W. J. Beenakker, Phys. Rev. B **44**, 1646 (1991).
- ³⁵ D. V. Averin, A. N. Korotkhov, and K. K. Likharev, Phys. Rev. B **44**, 6199 (1991).
- ³⁶ Yu. V. Nazarov, Physica B **189**, 57 (1993).
- ³⁷ S. A. Gurvitz, Phys. Rev. B **57**, 6602 (1998).
- ³⁸ J. von Delft and D. C. Ralph, Phys. Rep. **345**, 61 (2001).
- ³⁹ I. L. Aleiner, P. W. Brouwer, and L. I. Glazman, Phys. Rep. **358**, 309 (2002).
- ⁴⁰ Y. Alhassid, T. Rupp, A. Kaminski, and L. I. Glazman, Phys. Rev. B **69**, 115331 (2002).
- ⁴¹ A. Kaminski and L. I. Glazman, Phys. Rev. B **61**, 15927 (2000).
- ⁴² B. Dong, H. L. Cui, and X. L. Lei, Phys. Rev. B **69**, 035324 (2004).
- ⁴³ T. K. Ng and P. A. Lee, Phys. Rev. Lett. **61**, 1768 (1988).
- ⁴⁴ L. I. Glazman and M. E. Raikh, Pis'ma Zh. Eksp. Teor. Fiz. **47**, 378 (1988), [JETP Lett. **47**, 452 (1988)].
- ⁴⁵ R. A. Jalabert, A. D. Stone, and Y. Alhassid, Phys. Rev. Lett. **68**, 3468 (1992).
- ⁴⁶ D. A. Gorokhov and P. W. Brouwer, Phys. Rev. Lett **91**, 186602 (2003).
- ⁴⁷ D. A. Gorokhov and P. W. Brouwer, Phys. Rev. B **69**, 155417 (2004).
- ⁴⁸ D. Mozyrsky, L. Fedichkin, S. A. Gurvitz, and G. P. Berman, Phys. Rev. B **66**, 161313 (2002).